basis that riboflavin does not affect the acid–base titration curve of iron(II).[13] Current evidence[6] indicates that the stable tautomer of unreduced riboflavin is that illustrated in the Introduction (I). Such a species would have limited effectiveness as a coordinating agent. However, the radical anion of riboflavin has a tautomer form which is structurally similar (II) to the

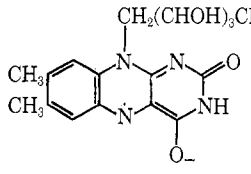

II

anion of 8-quinolinol, an extremely effective complexing agent.

The data in Table I indicate that this radical anion forms stable complexes with several metal cations in dimethyl sulfoxide. The highly charged metal ions cause greater peak potential shifts, implying that they form stronger complexes. If the formation of such complexes is assumed, the shift of the anodic peak potential should be more directly related to their stability. The shift in the cathodic peak also is dependent upon the rate of complex formation as well as the reversibility of the reduction reaction. On this basis the apparent order of stability is $La^{3+} = Y^{3+} > Th^{4+} > Ni^{2+} > Fe^{2+} > Ca^{2+} > Na^{+}$. The interaction between neutral riboflavin and metal ions appears to be insignificant, especially in view of its minimal effect on the reduction potential of iron(III).

The riboflavin anion is known to disproportionate in aqueous solution by the reaction[14]

$$2Rib^{-} \rightleftharpoons Rib + Rib^{2-} \quad (1)$$

In nonaqueous systems, the equilibrium for this reaction lies far to the left.[9] However, in the presence of the Y^{3+}, La^{3+}, and Th^{4+} ions the equilibrium appears to be shifted to the right in DMSO as the result of the formation of a more stable Rib^{2-} complex of the metal ions. This causes a significant decrease in the concentration of Rib^{-} accompanied by the formation of neutral riboflavin. The enhancement of the disproportionation of Rib^{-} by multivalent metal ions may occur through initial formation of bis complexes, $M(Rib^{-})_2$, which would then provide a convenient pathway for electron redistribution.

The interactions of metal ions with the various forms of riboflavin may depend in part upon the magnitudes of the charge on the riboflavin species and the metal ion. On this basis, neutral riboflavin would form weak complexes, while singly reduced riboflavin would interact strongly with highly charged metal cations. Highly charged metal ions also promote the disproportionation of the riboflavin anion to form a stronger complex with the doubly reduced Rib^{2-} species.

Acknowledgments.—This work was supported by the National Science Foundation under Grant No. GP-16114.

(13) T. R. Harkins and H. Freiser, *J. Phys. Chem.*, **63**, 309 (1959).

(14) A. Ehrenberg, F. Muller, and P. Hemmerich, *Eur. J. Biochem.*, **2**, 286 (1967).

CONTRIBUTION FROM THE PLASMA PHYSICS LABORATORY AND THE DEPARTMENT OF CHEMICAL ENGINEERING, PRINCETON UNIVERSITY, PRINCETON, NEW JERSEY 08540

The Stoichiometry and Kinetics of the Thermal Decomposition of Molten Anhydrous Lithium Nitrite[1]

BY A. K. K. LEE AND E. F. JOHNSON*[2]

Received March 19, 1971

A semiflow batch reactor has been used to study the thermal decomposition of molten anhydrous lithium nitrite at 250, 300, and 350°. The gaseous products of decomposition from a thin quiescent layer of molten nitrite were swept out of the reactor by a steady flow of argon gas. Kinetic curves of both the gas phase and the molten phase were obtained. The observed rate of overall nitrite decomposition can be represented by a first-order rate equation with the following rate constants: $k = (1.10 \pm 0.05) \times 10^{-6}$ sec^{-1} at 250°, $k = (1.30 \pm 0.07) \times 10^{-6}$ sec^{-1} at 300°, and $k = (1.25 \pm 0.07) \times 10^{-6}$ sec^{-1} at 350°. Individual reaction steps are proposed, which lead to the key reactions

$$3LiNO_2 \rightleftharpoons LiNO_3 + Li_2O + 2NO$$
$$2LiNO_2 \rightleftharpoons Li_2O + N_2O + O_2$$
$$2LiNO_2 + 2NO \longrightarrow 2LiNO_3 + N_2$$
$$2LiNO_3 \rightleftharpoons 2LiNO_3 + O_2$$

The observed overall stoichiometries of decomposition are consistent with combinations of these reactions.

Introduction

Considerable efforts have been made to study the thermal decomposition of molten nitrates and nitrites because the thermal stability and the rate of decomposition of these salts are important factors in molten salt technologies. Surveys[3,4] of the thermal decomposition of nitrates and nitrites indicate that the earlier studies of the decomposition of nitrites are limited to the iden-

(1) This work was supported in part by U. S. Atomic Energy Commission Contract AT(30-1)-1238.

(2) To whom correspondence should be addressed at the Plasma Physics Laboratory, Princeton University.

(3) L. E. Gastwirt and E. F. Johnson, "The Thermal Decomposition of Lithium Nitrate," Report MATT-98, Princeton Plasma Physics Laboratory, Princeton, N. J., 1961.

(4) A. K. K. Lee, Ph.D. Thesis, Princeton University, 1968.

tification of the products of decomposition and the elucidation of the stoichiometry of decomposition from equilibrium studies. Only in recent years have rate measurements been made in the thermal decomposition of alkali metal and alkaline earth metal nitrites.[5,6]

Fused lithium nitrite and lithium nitrate and mixtures of these two salts have been considered to be promising breeder blanket materials in a deuterium–tritium-fueled thermonuclear reactor.[7,8] Since lithium nitrite is one of the main decomposition products of lithium nitrate,[3,9,10] the study of thermal stability and the rate of decomposition of lithium nitrite will provide further understanding of the thermal stability and the kinetics of nitrite–nitrate mixtures.

The many earlier studies of the thermal decomposition of nitrites indicate that the system under study is a complex mixture of lithium nitrite, lithium nitrate, nitrogen, oxygen, and oxides of nitrogen. One of the inherent difficulties of these studies has been the occurrence of a variety of secondary reactions which follow the initial decomposition of nitrite. However, it is possible to reduce the extent of some secondary reactions to a negligible level by limiting the kinetic study to the first few per cent of the consumption of the pure initial charge in a closed vessel. But in a closed vessel the overall reaction is often complicated by heterogeneous reactions occurring at the gas–liquid phase boundary, with the result that the rates of some reactions are dependent on the surface area of the phase boundary. Therefore a semiflow batch method was chosen for the present study. By sweeping out the gaseous products from the surface of a stagnant pool of melt with an inert gas, heterogeneous reactions at the gas–liquid interface may be neglected if the concentrations of gaseous products are found to be extremely low in the inert-gas exit stream.

In the present case it was possible to follow the reaction in the molten phase by quenching identical systems at different times and analyzing the entire quenched residue. This procedure avoids the difficulties encountered in sampling melts at high temperatures in a closed reactor,[3] although it is rather costly in time and material. The composition of the gas phase can be followed readily by taking samples of the exit-gas stream.

Experimental Section

Materials.—All materials (except anhydrous lithium nitrite) used in this study were commercially available. Argon, nitrogen, oxygen, nitric oxide, nitrous oxide, nitrogen dioxide, nitrogen trioxide, and carbon dioxide were obtained from Matheson Co. High-purity argon 99.9995 minimum vol % and carbon dioxide of 99.995 minimum vol % were used. Lithium nitrite was prepared from the double decomposition of barium nitrite (minimum 98.7 wt %) and lithium sulfate (minimum 99.0 wt %). An aqueous solution of lithium nitrite was concentrated by vacuum distillation under an argon atmosphere. Lithium nitrite was then extracted from the concentrated solution by acetone and allowed to crystallize. The lithium nitrite monohydrate crystals were dried under high vacuum, with the temperature of the solid gradually increased to 100° over a period of 3 days. The resulting anhydrous solid was ground to powder in a drybox under an atmosphere of argon gas and then dried again. Its final composition was 98.89 wt % $LiNO_2$, 1.04 wt % $LiNO_3$, and 0.069 wt % Li_2O. The small amounts of nitrite and oxide contribute negligibly to the kinetics of decomposition of the nitrite because both components are formed rapidly in the initial stage of the decomposition.

Apparatus.—The kinetics of decomposition was studied using a semiflow batch system. The apparatus assembly consists of an argon gas cylinder, a dryer packed with anhydrous magnesium perchlorate, a microfilter for removing solids that might have been picked up by the gas stream from the dryer, a pressure regulator, a Bourdon pressure gauge and rotameter for measuring the flow rate of argon carrier gas, a reactor, a muffle furnace, a temperature controller, a mercury manometer, gas-collecting bulbs, a cold trap cooled by liquid nitrogen, an oil diffusion pump, and a vacuum pump. Analytical equipment consisted of a cycloidal mass spectrometer (Consolidated Electrodynamics Corp. Model CEC 21-620) and an apparatus with microazotometer for the gasometric determination of nitrite.

A cutaway view of the reactor is shown in Figure 1. The reactor, fabricated from hot-rolled Inconel to ensure high strength and resistance to corrosion by oxides of nitrogen, was kept small to ensure rapid heat-up to the reaction temperature and easy maintenance of uniform temperatures. It consisted essentially of two circular plates, the top one hollowed out in the form of a cone and the bottom constructed to hold a circular reaction dish. This dish was made of platinum to avoid attack by molten alkali nitrites and catalytic effects on the decomposition of molten nitrites.[11,12] The carrier gas entered the reactor around the perimeter of the reaction dish, swept toward the center, and flowed out through the top of the hollow cone, giving a flow characteristic approaching that of a plug-flow reactor.[4] A water-cooled quench plate attached to the bottom plate of the reactor and heating tapes wound around the bottom of the reactor ensured rapid cooling and heating of the reactor.

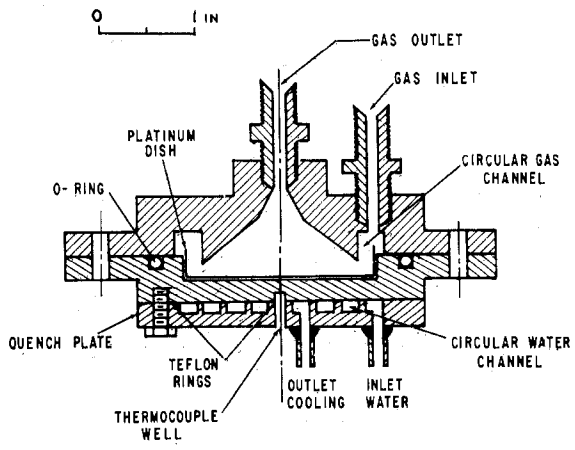

Figure 1.—Cutaway view of the reactor.

Procedure.—In a typical run about 2 g of anhydrous lithium nitrite was weighed accurately and transferred into the reaction dish under an atmosphere of argon to avoid moisture pickup. After sealing the reactor, the whole system was evacuated to remove any trapped gases. The argon flow was then set at 30 cm^3 (STP) min^{-1} at 5 psig and the reactor was inserted into the furnace for preheating. To avoid decomposition during preheating, the sample temperature was kept below 80° by circulating cooling water in the quench plate. After preheating for 2 hr, the heating tape was turned on to full power and the cooling water turned off. Timing of the reaction duration was started when the temperature first exceeded 100°, at which time all the

(5) P. I. Protsenko and E. A. Bordyushkova, *Zh. Neorg. Khim.*, **10**, 1215 (1965).

(6) P. I. Protsenko and E. A. Bordyushkova, *Zh. Fiz. Khim.*, **39**, 1978 (1965).

(7) E. F. Johnson, "Appraisal of Possible Stellarator Blanket Systems," Report NYO-7900, 1957.

(8) D. M. Gruen, "Fused Salts as Thermonuclear Reactor Breeding Blankets," Report ANL-5840, Argonne National Laboratory, Argonne, Ill., 1958.

(9) S. H. Cho and E. F. Johnson, "Kinetics of the Thermal Decomposition of Lithium Nitrate," Report MATT-324, Princeton Plasma Physics Laboratory, Princeton, N. J., 1964.

(10) E. A. Bordyushkova, P. I. Protsenko, and L. N. Venerovskaya, *Zh. Prikl. Khim. (Leningrad)*, **40**, 1438 (1967).

(11) T. M. Oza and B. R. Walawalker, *J. Indian Chem. Soc.*, **22**, 243 (1945).

(12) A. Peneloux, *C. R. Acad. Sci.*, **237**, 1082 (1953).

water in the quench plate had evaporated. The exit-gas stream was sampled at various time intervals and condensed in the cold trap.

Upon reaching reaction temperature, the reactions in the melt were terminated by quenching, and the reactor was removed from the furnace. After flushing with argon for about 15 min the reaction dish, with residue, was removed from the reactor and weighed immediately. The residue was dissolved in distilled water and stored in a volumetric flask for subsequent analysis.

The liquid nitrogen flask was removed from the cold trap and the condensed gas was allowed to expand into the gas bulbs. A sample of the gas mixture was taken the following day and the total volume, pressure, and temperature of the mixture were noted. All gas samples were analyzed by mass spectrometry.

The above description is for a reference run, *i.e.*, a run terminated the instant the sample reached reaction temperature. The same procedure was used in all other runs, except that reactions were allowed to proceed at the desired reaction temperature for durations of from 1 to 6 hr.

The amounts of nitrite, nitrate, and oxide in the residue solution were determined. The oxide was determined from the basicity of the solution by titration with a standardized hydrochloric acid solution using phenolphthalein indicator. Nitrate in the residue solution was reduced to nitric oxide in acid solution of ferrous sulfate and the excess ferrous ion was back-titrated with standard potassium dichromate solution to determine the amount of ferrous ion used in the reduction of nitrate.[13] Lithium nitrite was calculated by difference and checked by direct gasometric determination of nitrite using the quantitative generation of nitrogen gas from the reaction of the nitrite with sulfamic acid.[14]

Results

The decomposition of anhydrous lithium nitrite began at temperatures above 160° as indicated by the presence of nitric oxide in the argon sweep gas. The gaseous products in all the runs at 250, 300, and 350° consisted only of nitric oxide, nitrous oxide, nitrogen, and oxygen. No nitrogen dioxide was detected at these temperatures. However, in test runs at 450° nitrogen dioxide was detected, showing that nitrogen dioxide is produced in appreciable quantity only in high-temperature decompositions of the nitrite, as has been observed by Peneloux.[12]

The concentration–time curves of gaseous products shown in Figures 2–4 indicate that NO, N_2O, and N_2

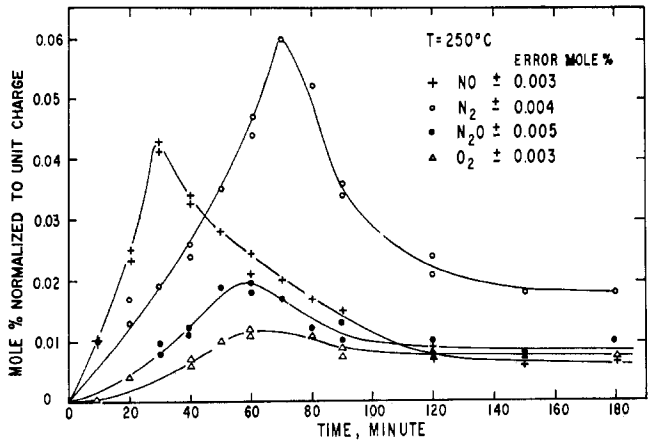

Figure 2.—Concentrations of gaseous products at 250°.

evolved rapidly at the beginning of decomposition. Their concentrations went through maxima and then fell to low steady values. The maxima for the O_2 concentrations were much less pronounced. At 250° the concentration peaks were spread out in time, the NO

(13) W. Leithe, *Anal. Chem.*, **20**, 1082 (1948).
(14) W. N. Carson, *ibid.*, **23**, 1016 (1951).

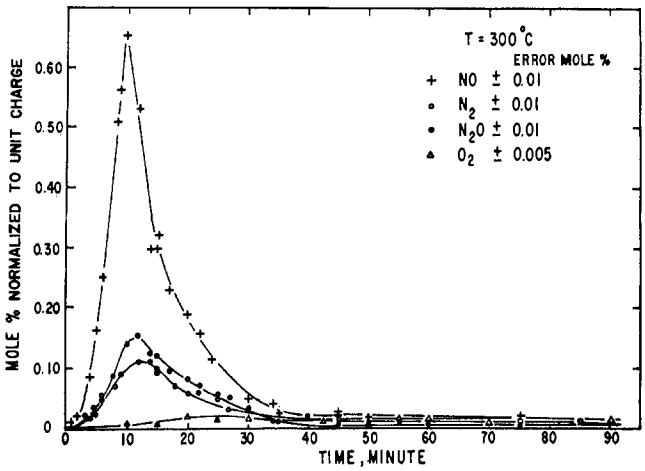

Figure 3.—Concentrations of gaseous products at 300°.

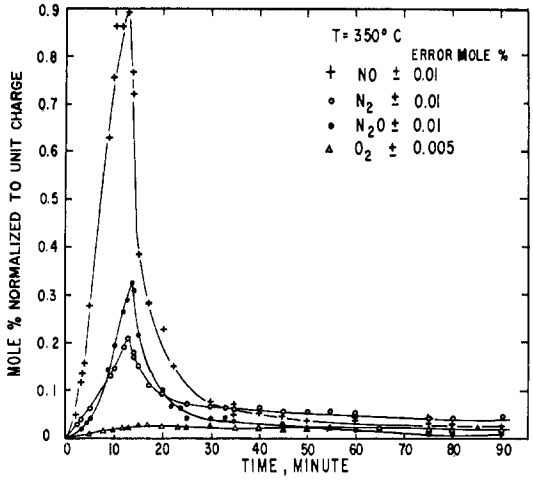

Figure 4.—Concentrations of gaseous products at 350°.

peak appearing first, followed by the N_2O and O_2 peaks and then the N_2 peak. At the two higher temperatures the peaks were much higher and sharper, and they all occurred in about 10–14 min. At these temperatures the N_2 peak became the third highest peak while it was the highest peak at 250°, indicating that the production of N_2 is strongly dependent on temperature.

The total volumes of each gas evolved at any particular time were obtained by integrating the concentration–time curves shown in Figures 2–4. These volumes are plotted as functions of time in Figures 5–7. Nitric

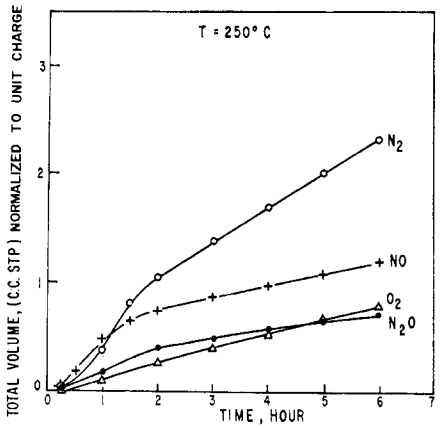

Figure 5.—Total volumes of gaseous products at 250°.

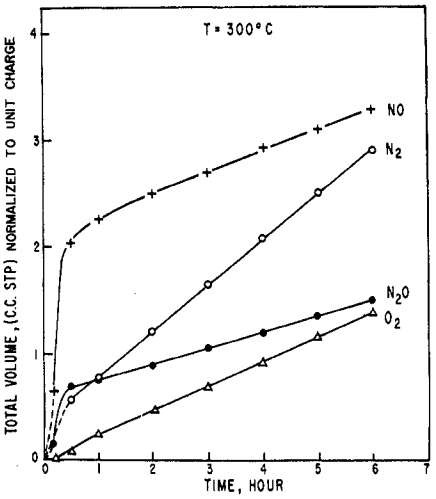

Figure 6.—Total volumes of gaseous products at 300°.

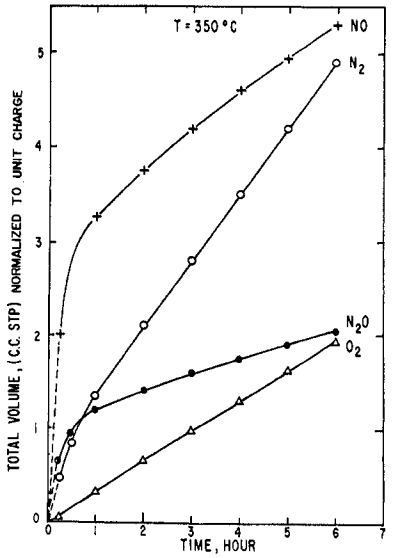

Figure 7.—Total volumes of gaseous products at 350°.

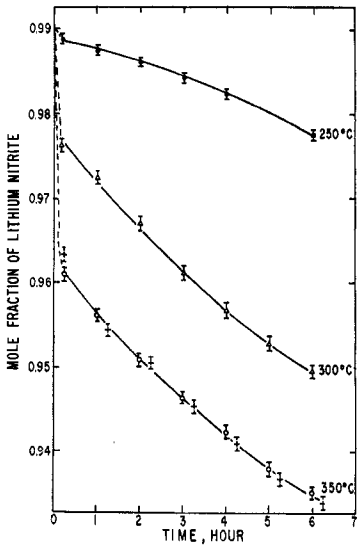

Figure 8.—Concentrations of lithium nitrite in the melt.

oxide was produced at the highest rate at the beginning of decomposition. After 2 hr, as the rate of decomposition became steady, nitrogen was produced at the highest rate. All of the steady gas production rates increased with increasing reaction temperature.

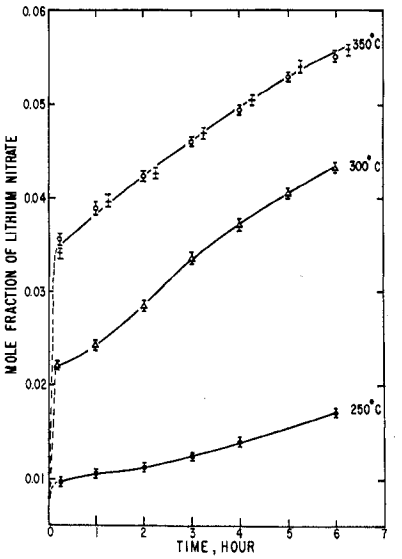

Figure 9.—Concentrations of lithium nitrate in the melt.

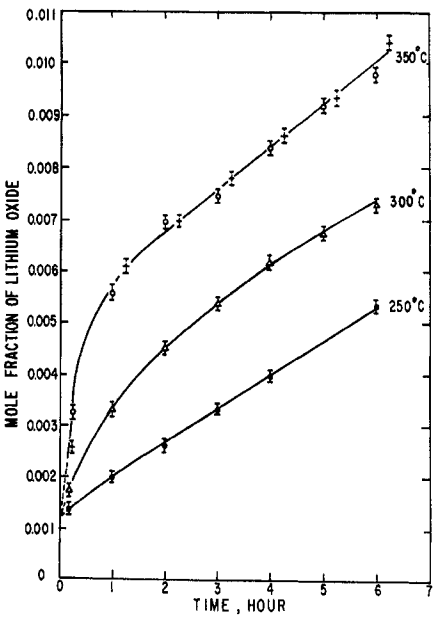

Figure 10.—Concentrations of lithium oxide in the melt.

The melt compositions of lithium nitrite, lithium nitrate, and lithium oxide, at reaction temperatures of 250, 300, and 350°, are shown graphically in Figures 8–10. The dashed lines in the figures indicate the periods of time when the temperatures of the samples were still below the reaction temperature. Initially the decomposition of the nitrite was rapid, as indicated by the sharp drop in the mole fraction of lithium nitrite in the melt composition. Within 1 hr the rate of nitrite decomposition dropped to a low steady value. The same behavior, a high initial rate of decomposition followed by the stabilization of the nitrite decomposition during continued isothermal heating, has been observed by Protsenko and Bordyushkova.[5] The reproducibility of the kinetic curves is shown in Figures 8–10 by two series of runs at 350°.

Discussion

Reaction Steps.—Since the gas concentrations at the gas–liquid interface are very low (even the highest peak of NO concentration is less than 1 mol % at 350°), the

amount of reaction occurring at the interface zone or in the gas phase is negligible in comparison with the amount in the bulk of the melt. Thus the reactions of lithium nitrite decomposition are considered to be homogeneous reactions between the dissolved gas phase and the melt.

From the time variation of gas composition and melt composition over a reaction time of 6 hr, the major steps in the thermal decomposition of lithium nitrite appear to be as follows.

The rapid initial stage consists of two steps: first, the decomposition of lithium nitrite to lithium oxide, nitric oxide, and oxygen; and, second, the recombination of the oxygen with the nitrite to form lithium nitrate

$$2LiNO_2 \rightleftharpoons Li_2O + 2NO + O \quad (1)$$

$$LiNO_2 + O \rightleftharpoons LiNO_3 \quad (2)$$

Overall, the initial reaction is

$$3LiNO_2 \rightleftharpoons Li_2O + LiNO_3 + 2NO \quad (3)$$

The first step is similar to the single-step mechanism suggested by earlier investigators[5,11,15,16]

$$2MNO_2 \rightleftharpoons M_2O + NO + NO_2 \quad (4)$$

where M is a monovalent metal and temperatures are high enough to ensure formation of the dioxide.

Next the nitrite decomposes to nitrous oxide and oxygen

$$2LiNO_2 \rightleftharpoons Li_2O + N_2O + O_2 \quad (5)$$

Nitrogen is formed by the nearly irreversible reaction between NO and nitrite

$$2LiNO_2 + 2NO \longrightarrow 2LiNO_3 + N_2 \quad (6)$$

Finally from the rising concentration of nitrate in the melt, oxygen is produced *via*

$$2LiNO_3 \rightleftharpoons 2LiNO_2 + O_2 \quad (7)$$

Thus the key stoichiometric reactions are (3), (5), (6), and (7). The peaks in the concentration–time curves of NO, N_2, N_2O, and O_2 in Figures 2–4 correspond to the relative predominance of these reactions. The initial fast rate of nitrite decomposition results in the production of gaseous products in the melt. As reactions proceed, the accumulation of these products in the melt quickly increases the importance of the reverse reactions, which then stabilize the decomposition of the nitrite.

Stoichiometry.—The thermal decomposition of lithium nitrite appears to follow different overall stoichiometries at different temperatures and at different melt compositions. The proportions of lithium nitrite consumed and the amounts of lithium nitrate and lithium oxide produced showed three distinct sets of stoichiometric ratios, namely, 10:4:3, 8:4:2, and 5:3:1, as indicated in Table I. The first set predominates at 250° and the last set at 300 and 350°. The other set occurs at the end of the 250° runs and at the beginning of the higher temperature runs.

Table II shows the corresponding stoichiometric ratios for the evolved gases during the steady-rate periods of decomposition. These ratios were computed from the slopes of the curves in Figures 5–7.

(15) T. M. Oza and M. S. Shah, *J. Indian Chem. Soc.*, **20**, 261 (1943).
(16) T. M. Oza, *ibid.*, **22**, 173 (1945).

Table I
Stoichiometric Ratios of Lithium Nitrite Decomposition

Δt, min	mol/g of charge Δ[LiNO2]	Δ[LiNO3]	Δ[Li2O]	Δ[LiNO2]:Δ[LiNO3]:Δ[Li2O]
		250°		
50	39	15	12	10:3.9:3.1
110	75	28	23	10:3.8:3.1
170	132	51	37	10:3.9:2.8
230	181	70	48	10:3.9:2.7
350	296	137	74	8:3.7:2.0
		300°		
50	87	40	29	10:4.6:3.4
110	208	118	51	8:4.5:2.0
170	366	212	67	5:2.9:0.9
230	457	277	82	5:3.0:0.9
290	544	341	92	5:3.1:0.9
350	612	390	103	5:3.2:0.8
		350°		
60	207	102	66	10:5.0:3.0
120	298	157	82	8:4.2:2.2
180	422	236	97	5:2.8:1.2
240	540	300	112	5:2.8:1.0
300	650	365	125	5:2.8:1.0
360	723	393	145	5:2.7:1.0

Table II
Stoichiometric Ratios of Evolved Gases
(Steady-Rate Decomposition of Lithium Nitrite)

Gas	250° Slope	250° Ratio	300° Slope	300° Ratio	350° Slope	350° Ratio
NO	0.220	4.4	0.400	4.2	0.760	7.0
N_2	0.652	13.1	0.855	9.0	1.440	13.3
N_2O	0.149	3.0	0.291	3.1	0.320	2.9
O_2	0.264	5.3	0.459	4.8	0.648	6.0

If the four key reactions (3), (5), (6), and (7) are written to produce the observed gas ratios for 250°, namely, 4:13:3:5 for $NO:N_2:N_2O:O_2$, the overall reaction is

$$73LiNO_2 = 37LiNO_3 + 18Li_2O + 4NO + 13N_2 + 3N_2O + 5O_2 \quad (8)$$

The corresponding stoichiometric ratios for the lithium compounds are therefore 73:37:18 or 8.0:4.1:1.0 in excellent agreement with those observed for the last 2 hr of the decomposition.

Similarly for 300°, where the gas ratios approximate 4:9:3:5, the stoichiometric coefficients for the respective lithium compounds are 53:25:14 or 5.0:2.4:1.3 in good agreement with the observed ratios. For 350° at gas ratios of 7:13:3:6 the melt coefficient ratios are 75.5:36.5:19.5 or 5.0:2.4:1.3, identical with those at 300°.

Overall Rate Constants.—The postulated chemistry for the thermal decomposition of lithium nitrite would suggest that the observed rates of the decomposition would be second order in nitrite composition. However, they can be quite well approximated by either simple first-order or second-order kinetics over the steady-rate course of the decomposition. Figure 11 shows the rate data in terms of the integrated form of the first-order rate equation, *viz.*

$$\ln x = \ln x_0 - kt \quad (9)$$

where x is the mole fraction of lithium nitrite, k is the rate constant, t is the time, and the subscript zero indicates the initial concentration.

The overall rate constants determined from the slopes in Figure 11 are $k = (1.10 \pm 0.05) \times 10^{-6}$ sec^{-1} at

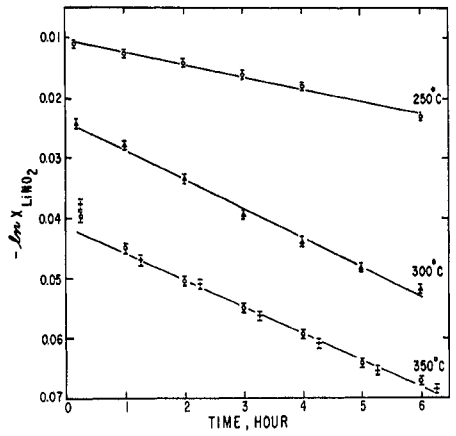

Figure 11.—First-order rate equation plots for the decrease of lithium nitrate.

250°, $k = (1.30 \pm 0.07) \times 10^{-6}$ sec^{-1} at 300°, and $k = (1.25 \pm 0.07) \times 10^{-6}$ sec^{-1} at 350°.

Although it is not possible to distinguish between the rate constants at 300 and 350°, it is clear that the rate of decomposition at 250° is slower. It is also clear that the initial rates of decomposition are very strongly dependent on temperature as indicated by the wide spread in the curves on Figure 11 despite identical starting compositions. Because of the complex nature of the nitrite decomposition, which involves consecutive, conjugate, and reversible reactions, there is no reason to expect that there would be a simple temperature dependency for the rate constants.

Stabilization of a $LiNO_2$–$LiNO_3$–Li_2O Mixture.—The initial rate of decomposition of pure nitrite is fast, but it decreases quickly to a low steady value depending on the rates of formation of nitrate and gaseous products. Using the prediction method of Lee and Johnson[17] the solubilities of the gaseous products in lithium nitrite are estimated to be of the order of 10^{-6} mol (cm^3 of melt)$^{-1}$ atm^{-1}. These solubilities are small, and consequently the concentrations of the gases in the melt rapidly approach the equilibrium concentrations and so depress the decomposition of nitrite.

The observed low rates of decomposition of lithium nitrite melts containing lithium nitrate and lithium oxide could be decreased further by pressurizing the melt with the gaseous products of the decomposition. By appropriate choice of gas composition and pressure the melt composition could be stabilized readily in the temperature range studied here.

(17) A. K. K. Lee and E. F. Johnson, *Ind. Eng. Chem., Fundam.*, **8**, 726 (1969).

CONTRIBUTION FROM THE DEPARTMENT OF CHEMISTRY, UNIVERSITY COLLEGE, CARDIFF, WALES, UNITED KINGDOM

The Electronic Spectra of the Hexahalo Anions of Osmium(IV) and Iridium(IV)

BY G. C. ALLEN, R. AL-MOBARAK,[1] G. A. M. EL-SHARKAWY,[1] AND KEITH D. WARREN*

Received June 1, 1971

The electronic spectra of the hexahalo anions of osmium(IV), OsX_6^{2-} (X = F, Cl, Br, I), and of iridium(IV), IrX_6^{2-} (X = F, Cl, Br), have been studied by diffuse reflectance between 4 and 50 kK. All the salts investigated show well-marked band systems of moderate intensity between 4 and 8 kK, which are interpreted as arising from transitions between the spin–orbit split components of the $^3T_{1g}$(Os(IV), d^4) and of the $^2T_{2g}$(Ir(IV), d^5) ground states, respectively. The spectra of the chloro, bromo, and iodo species are dominated by much stronger bands, assigned as Laporte-allowed charge-transfer transitions, which extend upward from between 10 and 20 kK and prevent the derivation of fitting parameters for the d–d excitations, but for the hexafluoro complexes the other d–d bands identified lead to the parameters $Dq = 2600$ cm^{-1}, $B = 500$ cm^{-1}, and $\xi = 2900$ cm^{-1}, for OsF_6^{2-}, and $Dq = 2700$ cm^{-1}, $B = 510$ cm^{-1}, and $\xi = 3300$ cm^{-1}, for IrF_6^{2-}. For OsF_6^{2-} the peak at 5.4 kK is ascribed to the $^3T_{1g}(\Gamma_1) \rightarrow {}^3T_{1g}(\Gamma_3, \Gamma_5)$ transition, and the weaker bands at 12.7 and 18.5 kK and the shoulder at 23 kK are assigned to the formally spin-forbidden excitations $^3T_{1g}(\Gamma_1) \rightarrow {}^1E_g$, $^1T_{2g}$, $^3T_{1g}(\Gamma_1) \rightarrow {}^5E_g$, and $^3T_{1g}(\Gamma_1) \rightarrow {}^1A_{1g}$, respectively. The stronger absorptions at about 30 and 42 kK are attributed to numerous spin-allowed $t_{2g}^4 \rightarrow t_{2g}^3e_g$ excitations, and the intense peak indicated slightly above 50 kK is attibuted to a $\pi \rightarrow t_{2g}$ charge-transfer transition. Similarly, for IrF_6^{2-} the prominent peak at 6.7 kK is assigned as the $^2T_{2g}(\Gamma_7) \rightarrow {}^2T_{2g}(\Gamma_8)$ excitation, and the less intense bands at 19.8 and 25.0 kK are attributed to the spin-forbidden transitions $^2T_{2g}(\Gamma_7) \rightarrow {}^4T_{1g}$ and $^2T_{2g}(\Gamma_7) \rightarrow {}^4T_{2g}$. The stronger broad bands at 30 and 38 kK again represent many spin-allowed transitions, here $t_{2g}^5 \rightarrow t_{2g}^4e_g$, while the Laporte-allowed $\pi \rightarrow t_{2g}$ band appears at 47.8 kK. From these data a measure of the extent of covalency for the OsF_6^{2-} and IrF_6^{2-} anions may be deduced, but for all the complexes the value of the effective spin–orbit coupling constant may be estimated from the low-energy bands, thus yielding some indication of this effect. The degree of covalency is found in both cases to increase in the sense $MF_6^{2-} < MCl_6^{2-} < MBr_6^{2-} < MI_6^{2-}$, but for the fluoro anion is found, predictably, to be appreciably smaller than for the corresponding Os(V) and Ir(V) species. Finally, consideration is given to the factors influencing the intensities and bandwidths of the low-energy transitions (and to the effects produced by the change of cation), and the derived ξ values are used for the calculation of relativistically corrected optical electronegativities.

Introduction

Although the M(V) and M(VI) hexahalo species of the 5d elements W to Pt are exemplified only by hexafluoro derivatives, many M(IV) hexahalo compounds are known, and numerous spectroscopic studies have been reported. Thus, the chloro, bromo, and iodo complexes of Os(IV) and the chloro and bromo derivatives of Ir(IV) have been studied in solution by Jørgensen,[2] and most of the intense bands which occur from between 10 and 20 kK upward were assigned as

(1) Ph.D. students supported by the Royal Saudi Arabian Government.

(2) C. K. Jørgensen, *Mol. Phys.*, **2**, 309 (1959).